Inorg. Chem. **2008**, *47*, 7972−7982

Synthesis, X-ray Crystallographic, and NMR Characterizations of Platinum(II) and Platinum(IV) Pyrophosphato Complexes†

Robert J. Mishur,‡ Chong Zheng,‡ Thomas M. Gilbert,‡ and Rathindra N. Bose*,‡,§

Department of Chemistry and Biochemistry, Northern Illinois University, DeKalb, Illinois 60115, and Departments of Chemistry & Biochemistry and of Biomedical Sciences, Ohio University, Athens, Ohio 45701

Received February 5, 2008

A series of mononuclear *cis*-diamineplatinum(II) pyrophosphato complexes containing ammine (am), *trans*-1,2-cyclohexanediamine (dach), and 1,2-ethanediamine (en) as the amine ligands were synthesized and characterized by ^{31}P and ^{195}Pt NMR spectroscopy. Chemical shifts of ^{31}P NMR resonances of these completely deprotonated complexes appear at 2.12, 1.78, and 1.93 ppm, indicating a coordination chemical shift of at least 8 ppm. The ^{195}Pt NMR chemical shifts for the am and dach complexes were observed at −1503 and −1729 ppm. The complexes are highly stable at neutral pH; no aquation due to the release of either phosphate or amine ligands was observed within 48 h. Furthermore, no partial deligation of the pyrophosphate ligand was detected within several days at neutral pH. At lower pH, however, release of a pyrophosphate ion was observed with concomitant formation of a bridged pyrophosphatoplatinum(II) dinuclear complex. The extended crystal structure containing the dach ligand revealed a zigzag chain stacked in a head-to-tail fashion. Moreover, two zigzag chains are juxtaposed in a parallel fashion and supported by additional hydrogen bonds reminiscent of DNA structures where two strands of DNA bases are held by hydrogen bonds. Theoretical calculations support the notion that the two dinuclear units are held together primarily by hydrogen bonds between the amine and phosphate moieties. Platinum(II) pyrophosphato complexes were readily oxidized by hydrogen peroxide to yield *cis*-diamine-*trans*-dihydroxopyrophosphatoplatinum(IV) complexes. Two of these complexes, containing am and en, were characterized by X-ray crystallography. Notable structural features include Pt−O (phosphate) bond distances of 2.021−2.086 Å and departures from 180° in *trans*-HO−Pt−OH bond angles, >90° in O−Pt−O, and >90 ° in *cis*-N−Pt−N bond angles. The departure in the *trans*-HO−Pt−OH angle is more pronounced in the 1,2-ethanediamine complex compared to the dach analogue because of the existence of two molecules possessing enantiomeric conformations within the asymmetric unit. ^{31}P NMR spectra exhibited well-resolved ^{195}Pt satellites with coupling constants of 15.4 Hz for the ammine and 25.9 Hz for both the 1,2-ethanediamine and *trans*-1,2-cyclohexanediamine complexes. The ^{195}Pt NMR spectrum of the ammine complex clearly showed coupling with two equivalent N atoms.

Introduction

The last 3 decades have witnessed an explosive growth in the metallobiochemistry of platinum(II) and platinum(IV) complexes because of the tremendous success of *cis*-diamminedichloroplatinum(II) (cisplatin) for the treatment of a variety of cancers.[1−3] In order to find more effective chemotherapeutics with reduced toxicity, many new platinum complexes have been synthesized and tested for their anticancer activities. These new complexes contain a variety of replaceable nonamine ligands for DNA binding as well as nonreplaceable amine ligands for better cellular uptake.[4,5] A thorough analysis of the literature supports the assertion

* To whom correspondence should be addressed: E-mail: bose@ohio.edu.

† This work was done at Northern Illinois University.

‡ Northern Illinois University.

§ Ohio University.

(1) Bose, R. N. *Mini-Rev. Med. Chem.* **2002**, *2*, 103–111.

(2) Wang, D.; Lippard, S. J. *Nat. Rev. Drug Discovery* **2005**, *4* (4), 307–320.

(3) Hall, M. D.; Hambley, T. G. *Coord. Chem. Rev.* **2002**, *232*, 49–67.

(4) (a) Quintal, S. M. O.; Qu, Y.; Quiroga, A. G.; Moniodis, J.; Nogueira, H. I. S.; Farrell, N. *Inorg. Chem.* **2005**, *44*, 5247–5253. (b) Kidani, Y.; Inagaki, K.; Iigo, M.; Hoshi, A.; Kuretani, K. *J. Med. Chem.* **1978**, *21* (12), 1315–1318.

10.1021/ic800237a CCC: $40.75
Published on Web 08/09/2008

that successful compounds are those that usually contain replaceable carboxylate ligands.[6,7] Furthermore, these compounds display much reduced rates of aquation and slow DNA binding properties compared to chloroplatinum(II) complexes.[8,9] Interestingly enough, these successful compounds contain hard bases as ligands coordinated to the soft acid, platinum(II). Besides carboxylato compounds and carbonatoplatinum(II)[10] and phosphonatoplatinum(II) complexes,[11] other soft−hard combinations also displayed excellent anticancer properties.

Despite tremendous efforts to replace cisplatin with more effective chemotherapeutics, coordination chemistry of phosphatoplatinum(II) and -platinum(IV) complexes and their antitumor activities remained largely unexplored. This is primarily due to the fact that early work on platinum(II) phosphato complexes usually resulted in phosphate-bridged dinuclear compounds.[12–15] Despite reports of excellent anticancer properties of some dinuclear phosphatoplatinum(II) complexes, further exploration of their applications were perhaps limited because of the poor solubility of these compounds in aqueous solutions. Although mononuclear pyro- and triphosphate as well as nucleoside 5′-triphosphate complexes were reported from our laboratory,[13,16–20] these compounds, especially pyro- and triphosphates, suffered phosphate hydrolysis in moderately acidic solutions, resulting in insoluble dinuclear products.[19,20] This Article describes the synthesis and characterization of a series of highly stable mononuclear platinum(II) and platinum(IV) complexes that indeed exhibit excellent antitumor activities in human ovarian cells.[21,22] In fact, in vitro tests of these compounds showed cytotoxicity in ovarian cells that are cross resistant to both cisplatin and carboplatin.[22] Furthermore, these compounds do not covalently bind DNA,[21,22] implying that the apoptotic mechanisms may be different from those proposed for cisplatin. Finally, we have characterized a pyrophosphato-bridged platinum(II) complex formed as a result of the aquation of the mononuclear complex by acid-catalyzed hydrolysis. To the best of our knowledge, this Article also reports the first examples of X-ray crystallographically characterized mononuclear phosphatoplatinum(IV) complexes. The structural formulas for the mononuclear platinum(II) and platinum(IV) phosphato complexes are shown in Figure 1.

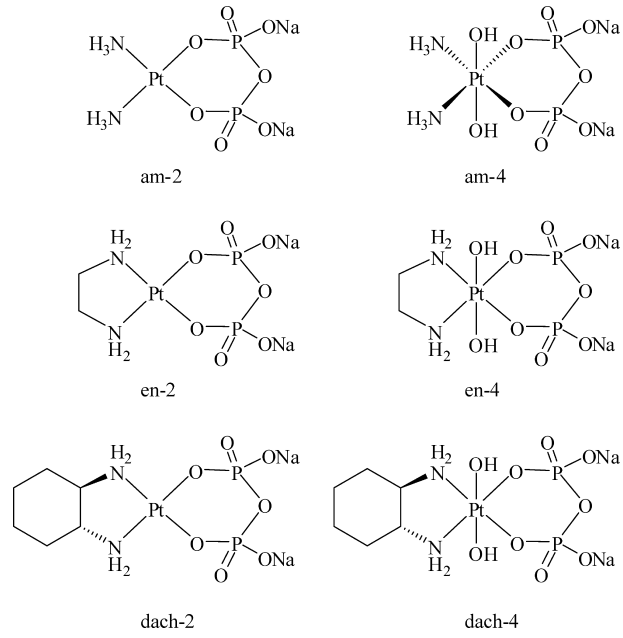

Figure 1. Chemical structures of platinum(II) and platinum(IV) pyrophosphato compounds.

Experimental Section

Reagents. Unless otherwise stated, all reagents were of the highest purity available from commercial vendors and were used without further purification. *cis*-Diamminedichloroplatinum(II) was synthesized following the method of Dhara.[23] Tetrasodium pyrophosphate, D_2O (99.9% atom), 1,2-ethanediamine, and *trans*-1,2-cyclohexanediamine were purchased from Aldrich. Platinum(II) pyrophosphate complexes were prepared following the method of Bose et al.[13] with modifications as elaborated below. Platinum(IV) complexes were synthesized by the oxidation of platinum(II) pyrophosphato complexes with hydrogen peroxide in the range of pH 7−9.

(5) Sundquist, W. I.; Lippard, S. J. *Coord. Chem. Rev.* **1990**, *100*, 293–322.
(6) (a) Calvert, A. H.; Harland, S. J.; Newell, D. R.; Siddik, Z. H.; Jones, A. C.; McElwain, T. J.; Raju, S.; Wiltshaw, E.; Smith, I. E.; Baker, J. M.; Peckham, M. J.; Harrap, K. R. *Cancer Chemother. Pharmacol.* **1982**, *9* (3), 140–147. (b) Harrap, K. R. *Cancer Treat. Rev.* **1985**, *12 (suppl. A)*, 21–33.
(7) (a) Mathe, G.; Kidani, Y.; Triana, K.; Brienza, S.; Ribaud, P.; Goldschmidt, E.; Ecstein, E.; Despax, R.; Musset, M.; Misset, J. L. *Biomed. Pharmacother.* **1986**, *40* (10), 372–376. (b) Soulie, P.; Raymond, E.; Brienza, S.; Cvitkovic, E. *Bull. Cancer* **1997**, *84* (6), 665–673.
(8) Knox, R. J.; Friedlos, F.; Lydall, D. A.; Roberts, J. J. *Cancer Res.* **1986**, *46*, 1972–1979.
(9) Jerremalm, E.; Pernilla, V.; Gunvor, A.; Griffiths, W. J.; Tomas, B.; Staffan, E.; Hans, E. *J. Pharm. Sci.* **2002**, *91* (10), 2116–2121.
(10) (a) Centerwall, C. R.; Goodisman, J.; Kerwood, D. J.; Toms, B. B.; Dubowy, R. L.; Dabrowiak, J. C. *J. Am. Chem. Soc.* **2005**, *127* (37), 12768–12769. (b) Centerwall, C. R.; Tacka, K. A.; Kerwood, D. J.; Goodisman, J.; Toms, B. B.; Dubowy, R. L.; Dabrowiak, J. C. *Mol. Pharmacol.* **2006**, *70* (1), 348–355.
(11) (a) Appleton, T. G.; Hall, J. R.; McMahon, I. J. *Inorg. Chem.* **1986**, *25* (6), 720–725. (b) Appleton, T. G.; Hall, J. R.; McMahon, I. J. *Inorg. Chem.* **1986**, *25* (6), 726–734.
(12) Stanko, J. A. In *Platinum Coordination Complexes in Cancer Chemotherapy*; Conners, T. A., Robert, J. J., Eds.; Springer-Verlag: New York, 1974; pp 24−26.
(13) Bose, R. N.; Viola, R. E.; Cornelius, R. D. *J. Am. Chem. Soc.* **1984**, *106*, 3336–3344.
(14) Appleton, T. G.; Berry, R. D.; Hall, J. R. *Inorg. Chim. Acta* **1982**, *64* (5), L229–L233.
(15) Wood, F. E.; Hunt, C. T.; Balch, A. L. *Inorg. Chim. Acta* **1982**, *67* (4), L19–L20.
(16) Bose, R. N.; Goswami, N.; Moghaddas, S. *Inorg. Chem.* **1990**, *29*, 3461–3467.
(17) Bose, R. N.; Slavin, L. L.; Cameron, J. W.; Luellen, D.; Viola, R. E. *Inorg. Chem.* **1993**, *32*, 1795–1802.
(18) Slavin, L. L.; Bose, R. N. *J. Chem. Soc., Chem. Commun.* **1990**, *18*, 1256–1258.
(19) Bose, R. N.; Cornelius, R. D.; Viola, R. E. *Inorg. Chem.* **1984**, *23*, 1181.
(20) Bose, R. N.; Cornelius, R. D.; Viola, R. E. *Inorg. Chem.* **1985**, *24*, 3989.
(21) Bose, R. N.; Mishur, R. J.; Yasui, L.; Gupta, S.; Maurmann, L. Monomeric Phosphoplatins as Anticancer Drugs. U.S. Patent and Trademark Office, 2007, Provisional Application 60/954,126. Bose, R. N. Effectiveness of Phosphoplatins towards cisplatin and carboplatin resistant cancer cells. U.S. Patent and Trademark Office, 2007, Provisional Application 60/973,926.
(22) Bose, R. N.; Maurmann, L.; Mishur, R.; Gupta, S.; Yasui, L.; Grayburn, W. S.; Hofstetter, H. *Proc. Natl. Acad. Sci. U.S.A.* **2008**, submitted for publication.
(23) Dhara, S. C. *Indian J. Chem.* **1970**, *8*, 193–194.

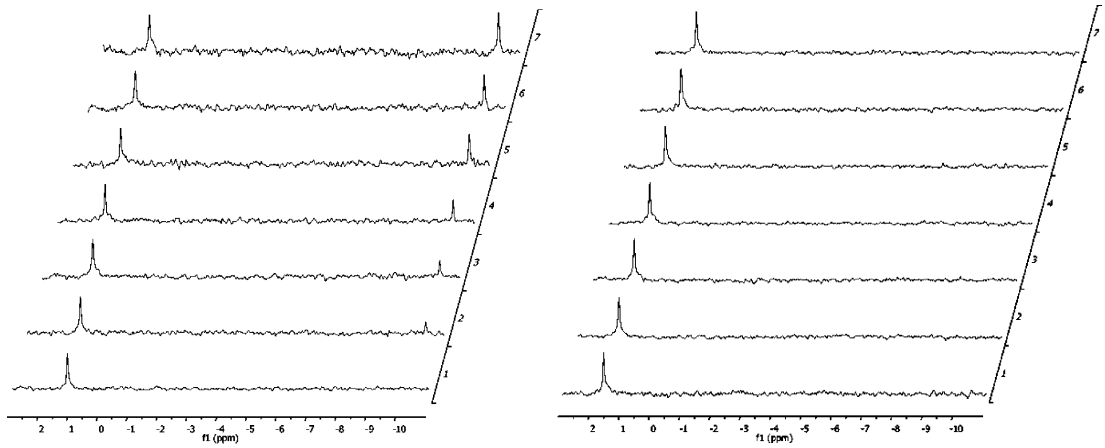

Figure 2. Hydrolysis of dach-2 (9.0 mM) monitored by ^{31}P NMR in 10% D_2O at pH 4.2 (left) and 7.0 (right) up to 6 days. The spectra were recorded at 1 day intervals starting on day 0 (bottom).

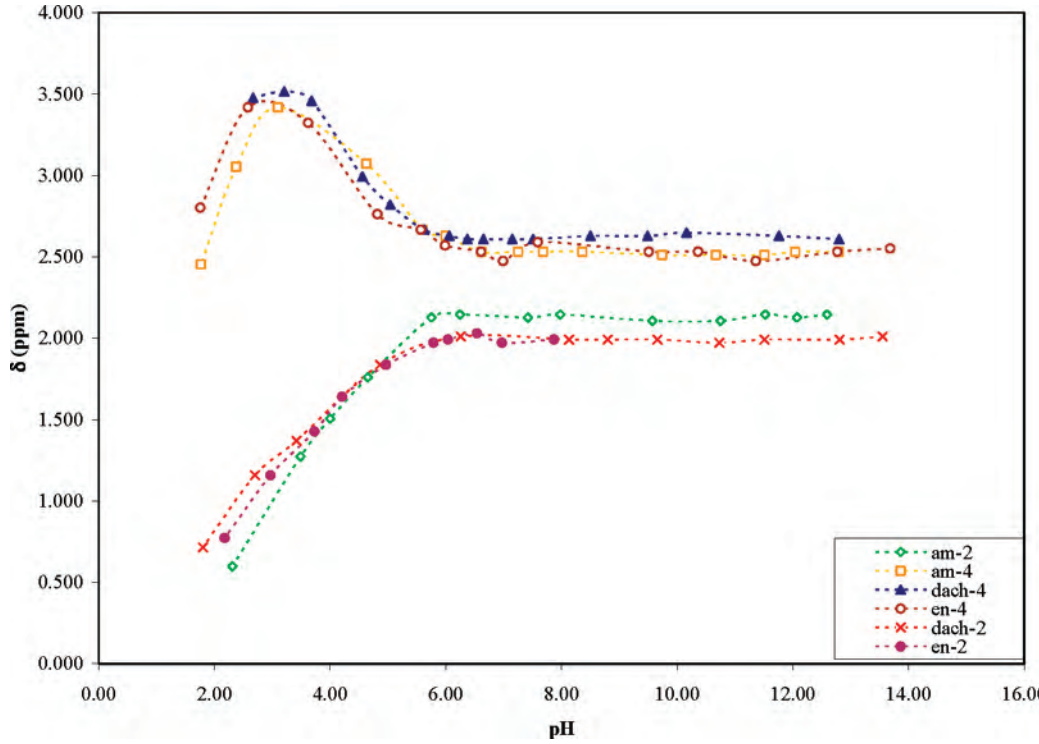

Figure 3. pH−^{31}P NMR chemical shift profiles of platinum(II) and platinum(IV) pyrophosphato complexes. Individual complexes were defined in the inset of the plot.

Synthesis. Diammine(dihydrogen pyrophosphato)platinum-(II) (am-2). Sodium pyrophosphate decahydrate (0.4 g) and 0.1 g of cisplatin were dissolved in 250 mL of distilled water (the pH was adjusted to pH 8), and the resulting mixture was incubated at 40 °C for 15 h. Following the incubation period, the solution was concentrated to 5−10 mL by rotary evaporation and filtered to remove any unreacted starting material. Lowering the pH to approximately 1.0 by the addition of 1 N HNO_3 precipitated the product as a light-yellow powder. Precipitation was completed by cooling on ice, and the product was isolated by vacuum filtration and washed with cold water and acetone. Yield of $[Pt(NH_3)_2(H_2P_2O_7)]$: 0.04 g (30%). The ^{31}P NMR spectrum displays a single peak at 2.12 ppm at pH 7.99.

***cis*-Diammine-*trans*-dihydroxo(dihydrogen pyrophosphato)-platinum(IV) (am-4; Figure 4).** Sodium pyrophosphate decahydrate (0.4 g) and 0.1 g of cisplatin were dissolved in 250 mL of distilled water. The pH of the mixture was adjusted to 8, and the mixture was incubated at 40 °C for 15 h. Following the incubation period, 1 mL of 30% H_2O_2 was added to the reaction mixture, and it was allowed to react for a further 3 h. The solution was then concentrated to 5−10 mL by rotary evaporation and filtered to remove any unreacted starting material. Lowering the pH to approximately 1.0 by the addition of 1 N HNO_3 precipitated the product as a light-yellow powder. Precipitation was completed by cooling on ice, and the product was isolated by vacuum filtration and washed with cold water and acetone. Yield of *cis*,*trans*-$[Pt(NH_3)_2(OH)_2(H_2P_2O_7)]$: 0.05 g (34%). The ^{31}P NMR spectrum displays a single peak at 2.32 ppm at pH 8.11 with a $^{195}Pt-^{31}P$ coupling constant of 15.4 Hz. The ^{195}Pt NMR spectrum shows a pentet at 1733 ppm with a $^{195}Pt-^{14}N$ coupling constant of 232 Hz.

1,2-Ethanediamine(dihydrogen pyrophosphato)platinum(II) (en-2). Sodium pyrophosphate decahydrate (0.4 g) and 0.1 g of dichloro(1,2-ethanediamine)platinum(II) were dissolved in 250 mL of distilled water. The pH of the mixture was adjusted to 8, and the mixture was incubated at 40 °C for 15 h. Following the incubation period, the solution was concentrated to 5−10 mL by

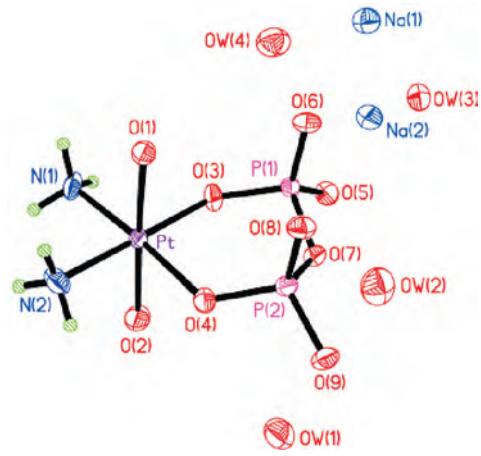

Figure 4. Crystal structure of am-4.

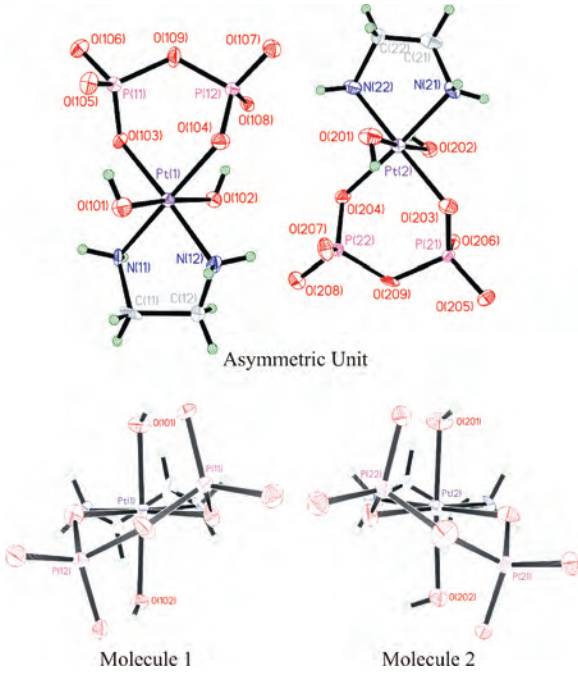

Figure 5. Crystal structure of en-4. The top part shows the relative orientation of the two molecules in the asymmetric unit. The bottom part demonstrates the different conformations of the two molecules viewed from the pyrophosphate side.

rotary evaporation and filtered to remove any unreacted starting material. Lowering the pH to approximately 1.0 by the addition of 1 N HNO_3 did not precipitate the product. The product was characterized in situ by ^{31}P NMR. A single peak with a $^{195}Pt-^{31}P$ coupling constant of 29.7 Hz is observed at 1.93 ppm in the ^{31}P NMR spectrum.

1,2-Ethanediamine-*trans*-dihydroxo(dihydrogen pyrophosphato)platinum(IV) (en-4; Figure 5). Sodium pyrophosphate decahydrate (0.4 g) and 0.1 g of dichloro(1,2-ethanediamine)platinum(II) were dissolved in 250 mL of distilled water. The pH of the mixture was adjusted to 8, and the mixture was incubated at 40 °C for 15 h. Following the incubation period, 1 mL of 30% H_2O_2 was added to the reaction mixture, and it was allowed to react for a further 3 h. The solution was then concentrated to 5−10 mL by rotary evaporation and filtered to remove any unreacted starting material. Lowering the pH to approximately 1.0 by the addition of 1 N HNO_3 precipitated the product as a light-yellow powder. Precipitation was completed by cooling on ice, and the product was isolated by vacuum filtration and washed with cold water and acetone. Yield of *trans*-$[Pt(C_2H_8N_2)(OH)_2(H_2P_2O_7)]$: 0.07 g (49%). The ^{31}P NMR spectrum displays a single peak at 2.30 ppm at pH 8.13 with a $^{195}Pt-^{31}P$ coupling constant of 25.9 Hz. The ^{195}Pt NMR spectrum showed a broad peak at 1582 ppm.

(*trans*-1,2-Cyclohexanediamine)(dihydrogen pyrophosphato)-platinum(II) (dach-2). Sodium pyrophosphate decahydrate (0.4 g) and 0.1 g of *cis*-dichloro(*trans*-1,2-cyclohexanediamine)platinum(II) were dissolved in 250 mL of distilled water. The pH of the mixture was adjusted to 8, and the mixture was incubated at 40 °C for 15 h. Following the incubation period, the solution was concentrated to 5−10 mL by rotary evaporation and filtered to remove any unreacted starting material. Lowering the pH to approximately 1.0 by the addition of 1 N HNO_3 precipitated the product as a light-yellow powder. Precipitation was completed by cooling on ice, and the product was isolated by vacuum filtration and washed with cold water and acetone. Yield of $[Pt(C_6H_{14}N_2)(H_2P_2O_7)]$: 0.05 g (38%). The ^{31}P NMR spectrum displays a single peak at 1.78 ppm at pH 7.93.

Crystals of the pyrophosphato-bridged dinuclear complex (dinuclear dach-2; Figure 6) were grown by layering a solution of 30 mM dach-2 in water (pH 10) with DMF in an NMR tube. Crystals were observed to grow at the interface in about 1 month.

(*trans*-1,2-Cyclohexanediamine)-*trans*-dihydroxo(dihydrogen pyrophosphato)platinum(IV) (dach-4). Sodium pyrophosphate decahydrate (0.4 g) and 0.1 g of *cis*-dichloro(*trans*-1,2-cyclohexanediamine)platinum(II) were dissolved in 250 mL of distilled water. The pH of the mixture was adjusted to 8, and the mixture was incubated at 40 °C for 15 h. Following the incubation period, 1 mL of 30% H_2O_2 was added to the reaction mixture, and it was allowed to react for a further 3 h. The solution was then concentrated to 5−10 mL by rotary evaporation and filtered to remove any unreacted starting material. Lowering the pH to approximately 1.0 by the addition of 1 N HNO_3 precipitated the product as a light-yellow powder. Precipitation was completed by cooling on ice, and the product was isolated by vacuum filtration and washed with cold water and acetone. Yield of *trans*-$[Pt(C_6H_{14}N_2)(OH)_2(H_2P_2O_7)]$: 0.07 g (52%). The ^{31}P NMR spectrum displays a single peak at 2.41 ppm at pH 7.95 with a $^{195}Pt-^{31}P$ coupling constant of 25.9 Hz. The ^{195}Pt NMR spectrum showed a broad peak at 1613 ppm.

Physical Measurements. Nuclear Resonance Spectroscopy. NMR measurements were carried out on either a Bruker 500 or 200 MHz instrument. ^{31}P NMR chemical shifts are reported with respect to 85% phosphoric acid, while ^{195}Pt NMR resonances are referenced with respect to H_2PtCl_6. Typically, ^{31}P NMR measurements were carried out at 81 or 224 MHz with a sweep width of 25 kHz by using a deuterium lock. A 90° pulse of 5 μs with a 1.0 s repetitive delay was applied to the solutions of phosphato complexes ~100 mM in D_2O. Following the application of pulses, free induction decays (FIDs) with 16K data points were collected. The FIDs were transformed by Fourier transformation with a 3.0 Hz line-broadening factor. Usually, 1000 FIDs were sufficient to generate signals with a S/N ratio > 10. ^{195}Pt NMR spectra were recorded from the same solutions referenced above for ^{31}P NMR measurements at a frequency of 43 MHz. Typical data acquisition parameters were similar to those of ^{31}P except that a 500 ms pulse repetition time and a sweep width of 25 kHz were selected. The smaller sweep width was selected to avoid a rolling baseline problem. However, wider sweep widths, >100 kHz, were covered by sequentially changing frequencies from a lower magnetic field to a higher magnetic field to ensure that no signals remained

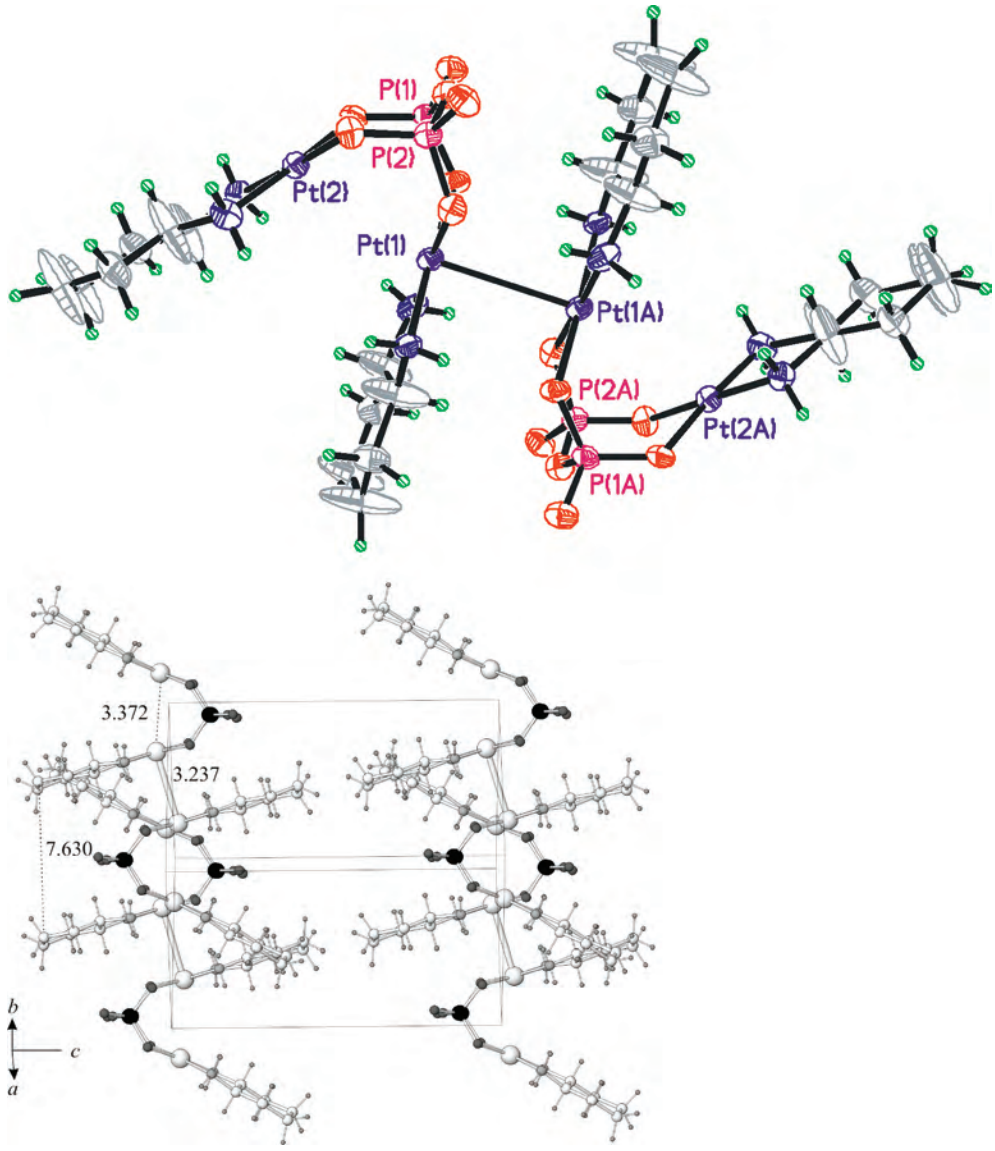

Figure 6. Crystal structure of dinuclear dach-2: (a, top) dinuclear molecule; (b, bottom) stacking of the dinuclear molecules along the (−1, 1, 0) direction.

undetected, and the folding effect was eliminated. Also, a line-broadening factor of 30 Hz was used during Fourier transformation.

Acidity Constant Measurements. Acidity constants for complexes were determined from chemical shift−pH profiles. Platinum complexes were dissolved in 0.1 M NaOH to a concentration of 10 mM. Nitric acid (0.1 M) was added to lower the pH, and aliquots were removed at various pHs. The concentration of platinum was kept within 5−10 mM for all samples. The chemical shifts (δ)−pH data exhibited clear biphasic profiles in some cases and were fitted to eq 1[16] or 2[24] depending on the monophasic or biphasic profiles characteristic of monoprotic or diprotic acids exhibited by these compounds.

$$\delta = \frac{\delta_1[H_3O^+]^2 + \delta_2 K_{a1}[H_3O^+] + \delta_3 K_{a1} K_{a2}}{[H_3O^+]^2 + K_{a1}[H_3O^+] + K_{a1}K_{a2}} \qquad (1)$$

In this equation, δ is the measured chemical shift and δ_1, δ_2, and δ_3 are chemical shifts of diprotic, monoprotic, and deprotonated forms of the complex. In some cases, the complexes existed in the monoprotic forms at the lowest possible pH in our experiments and exhibited monophasic δ−pH profiles. These profiles were fitted to eq 2.

$$\delta = \frac{\delta_2[H_3O^+] + \delta_3 K_{a2}}{[H_3O^+] + K_{a2}} \qquad (2)$$

X-ray Diffraction Measurements. Several crystals of each of am-4, en-4, and dinuclear dach-2 were indexed on a Bruker SMART CCD diffractometer using 40 frames with an exposure time of 20 s/frame. One crystal from each compound with good reflection quality was chosen for data collection. A total of 4991, 7441, and 9546 reflections were collected in the hemisphere of the reciprocal lattice for the three compounds. Of these reflections, 2337, 1820, and 4555 were unique with R(int) = 0.0222, 0.0176, and 0.0311, respectively. Empirical absorption corrections using the program *SADABS*[25] were applied to all reflections. The structures were

(24) Westermoreland, D. G.; Mathews, C. R. *J. Biol. Chem.* **1975**, *250*, 7456–7460.

(25) Sheldrick, G. M. *SHELXTL*, version 6.10; Bruker Analytical Instruments Inc.: Madison, WI, 2000.

solved with direct methods using the *SIR97* program.[26] Full matrix least-squares refinements on F^2 were carried out using the *SHELXTL* program.[27] The final agreement factors are R1 = 0.0233, 0.0183, and 0.0506 and wR2 = 0.0633, 0.0457, and 0.1360 ($I > 2\sigma$). All final structures were checked for additional symmetry with the MISSYM algorithm[28] implemented in the *PLATON* program suite.[29] No additional symmetry was found.

Computational Studies. All calculations were performed with the GAUSSIAN code.[30] Dinuclear dach-2 and its dimeric (tetranuclear) unit were modeled by substituting 1,2-ethanediamine (en) for the *trans*-1,2-cyclohexanediamine ligand. Three conformers of the monomer moiety were initially optimized without constraints at the BLYP/LANL2DZ level: one where both PtO_2P_2O rings adopted chair conformations, one where both rings adopted boat conformations, and one where one of each conformation was adopted. The boat/boat conformer proved most stable, but all three conformers lie within 10 kJ mol^{-1} of each other, so none is greatly preferred. Dimerization energies reported in the Results and Discussion section are with respect to the boat/boat conformer. The dimer model was constrained to C_i symmetry during optimizations for computational efficiency and to match the crystal structure.

The natures of stationary point structures were probed by analytical frequency analysis at the BLYP/LANL2DZ level. The structures were then reoptimized using the other models noted below. Dimerization energies were corrected using unscaled zero-point energies from the frequency analysis.

The BLYP[31] density functional theory (DFT) model and the MP2[32] perturbation theory model were used as coded in GAUSSIAN; the MPW1K DFT model was generated using IOp keywords.[33] The BLYP model was selected for the bulk of the calculations because work from Truhlar suggests it is among the best DFT models for transition-metal compounds.[34,35] The other models were chosen to probe the energetics of hydrogen bonding, as detailed below. Cartesian coordinates (BLYP/LANL2DZ) of the dinuclear and tetranuclear units are available as Supporting Information.

Results

Synthesis and NMR Characterization. Reactions of sodium pyrophosphate with *cis*-diaminedichloroplatinum(II) complexes at pH 7−9 readily formed respective *cis*-diamine(pyrophosphato)platinum(II) complexes as evidenced from ^{31}P NMR spectroscopy. Each of these pyrophosphato complexes exhibited a single ^{31}P NMR resonance with chemical shifts in the range 1.78−2.12 ppm. These chemical shifts are 9−11 ppm downfield compared to the free pyrophosphate ligand, consistent with the observed coordination chemical shifts for phosphate chelates reported in the literature.[36] Monodentate pyrophosphato complexes were not detected in the final products, as revealed by the absence of the expected two sets of doublets.

Table 1. Chemical Shifts for Deprotonated Platinum(II) and Platinum(IV) Pyrophosphato Complexes

complex	δ ^{31}P, ppm	δ ^{195}Pt, ppm	J_{P-Pt}, Hz	J_{Pt-N}, Hz
am-2	2.12	−1503	23.44	
dach-2	1.78	−1729	25.03	
en-2	1.93	N/A	29.73	
am-4	2.32	1733	15.38	232
dach-4	2.41	1613	25.91	
en-4	2.35	1582	25.91	

At neutral pH, these platinum(II) pyrophosphato complexes are remarkably stable. Figure 2 shows the ^{31}P NMR spectra of dach-2 at two different pHs over 6 days at 1 day time intervals. As can be seen from Figure 2, at neutral pH, the complex did not suffer any deligation due to the loss of either an amine or a pyrophosphate ligand. However, slow deligation due to the release of the pyrophosphate ligand was evident at pH 4.2 by the appearance of the free pyrophosphate signal at −10.3 ppm. At the same time, an insoluble pyrophosphato-bridged dinuclear platinum(II) product was formed, which was separated and characterized by X-ray crystallography for the dach complex as described below.

The platinum(II) pyrophosphato complexes were oxidized by H_2O_2 to yield *cis*-diamine-*trans*-dihydroxopyrophosphatoplatinum(IV) complexes. This oxidation process was remarkably selective, as evidenced by the formation of a single pyrophosphatoplatinum(IV) complex in each case, based on the ^{31}P NMR data. Furthermore, addition of an ammonia buffer (pH 9.5) to the reaction did not yield any new products. Two of the three platinum(IV) complexes afforded high-quality single crystals and were characterized by X-ray crystallography as discussed below.

Table 1 lists the ^{31}P and ^{195}Pt NMR chemical shifts of the completely deprotonated complexes. In some cases, ^{31}P NMR spectra exhibited satellites due to the couplings with ^{195}Pt nuclei (33.4% abundance). The coupling constants lie in the range 15.4−25.9 Hz for platinum(IV) complexes. ^{31}P NMR spectra of these compounds exhibit pH-dependent chemical shifts. Figure 3 shows pH−chemical shift profiles of the complexes. Note that platinum(IV) complexes exhibit higher chemical shifts than the corresponding platinum(II) analogues especially in the lower pH region. The pH−chemical shift data were used to estimate the pK_a values of these complexes. Table 2 lists the estimated pK_a values of these compounds

(26) Altomare, A.; Burla, M. C.; Camalli, M.; Cascarano, G. L.; Giacovazzo, C.; Guagliardi, A.; Moliterni, A. G. G.; Polidori, G.; Spagna, R. *J. Appl. Crystallogr.* **1999**, *32*, 115.
(27) Le Page, Y. *J. Appl. Crystallogr.* **1987**, *20*, 264.
(28) Spek, A. L. *Acta Crystallogr., Sect. A: Found. Crystallogr.* **1990**, *46*, C34.
(29) Whangbo, M.-H.; Hoffmann, R. *J. Am. Chem. Soc.* **1978**, *100*, 6093.
(30) Frisch, M. J.; Trucks, G. W.; Schlegel, H. B.; Scuseria, G. E.; Robb, M. A.; Cheeseman, J. R.; Zakrzewski, V. G.; Montgomery, J. A., Jr.; Stratmann, R. E.; Burant, J. C.; Dapprich, S.; Millam, J. M.; Daniels, A. D.; Kudin, K. N.; Strain, M. C.; Farkas, O.; Tomasi, J.; Barone, V.; Cossi, M.; Cammi, R.; Mennucci, B.; Pomelli, C.; Adamo, C.; Clifford, S.; Ochterski, J.; Petersson, G. A.; Ayala, P. Y.; Cui, Q.; Morokuma, K.; Malick, A D.; Rabuck, K. D.; Raghavachari, K.; Foresman, J. B.; Cioslowski, J.; Ortiz, J. V.; Baboul, A. G.; Stefanov, B. B.; Liu, G.; Liashenko, A.; Piskorz, P.; Komaromi, I.; Gomperts, R.; Martin, R. L.; Fox, D. J.; Keith, T.; Al-Laham, M. A.; Peng, C. Y.; Nanayakkara, A.; Challacombe, M.; Gill, P. M. W.; Johnson, B.; Chen, W.; Wong, M. W.; Andres, J. L.; Gonzalez, C.; Head-Gordon, M.; Replogle, E. S.; Pople, J. A. *Gaussian 98*, revision A.11.4; Gaussian, Inc.: Pittsburgh, PA, 1998.
(31) (a) Becke, A. D. *Phys. Rev. A* **1988**, *38*, 3098–3100. (b) Lee, C.; Yang, W.; Parr, R. G. *Phys. Rev. B* **1988**, *37*, 785–789.
(32) Moller, C.; Plesset, M. S. *Phys. Rev.* **1934**, *46*, 618–622.
(33) Lynch, B. J.; Truhlar, D. G. *J. Phys. Chem. A* **2001**, *105*, 2936–2941.
(34) (a) Schultz, N. E.; Zhao, Y.; Truhlar, D. G. *J. Phys. Chem. A* **2005**, *109*, 4388–4403. (b) Schultz, N. E.; Zhao, Y.; Truhlar, D. G. *J. Phys. Chem. A* **2005**, *109*, 11127–11143.
(35) (a) Zhao, Y.; Truhlar, D. G. *J. Chem. Theory. Comput.* **2007**, *3*, 289–300. (b) Zhao, Y.; Truhlar, D. G. *J. Chem. Theory. Comput.* **2006**, *2*, 1009–1018. (c) Zhao, Y.; Truhlar, D. G. *J. Chem. Theory. Comput.* **2005**, *1*, 415–432.
(36) Cornelius, R. D.; Hart, P. A.; Cleland, W. W. *Inorg. Chem.* **1977**, *16* (11), 2799–2805.

Table 2. Calculated pK_a Values for Platinum(II) and Platinum(IV) Pyrophosphato Complexes[a]

compound	pK_{a1}	pK_{a2}	δ_1	δ_2	δ_3
am-2	2.9 ± 0.3 (3.8 ± 0.1)	4.7 ± 0.2	0.37 (0.62)	1.49	2.14
en-2	2.2 ± 0.1	4.4 ± 0.1	0.44	1.35	1.99
dach-2	2.6 ± 0.2 (3.3 ± 0.1)	4.4 ± 0.2	0.54 (0.77)	1.40	1.99
am-4	2.0 ± 0.1	4.7 ± 0.1	1.735	3.55	2.53
en-4	<2	4.3 ± 0.1	0.0	3.54	2.53

[a] The chemical shifts, δ_1 and δ_2, for the diprotic and monoprotic acid forms were genered from the computer fit of eq 1. The values in parentheses were obtained based on eq 2, assuming a monoprotic behavior where the values of δ_2 were exactly the same as experimentally determined chemical shifts for the completely deprotonated forms listed under δ_3.

based on limited data. Most of these complexes show a biphasic profile, with an initial increase in the chemical shift with an increase in the pH, followed by a slight decrease in the chemical shift upon a further increase in the pH. These biphasic profiles certainly correspond to two protonation/deprotonation sites in the complexes and are consistent with the formulation $[Pt(H_2P_2O_7)(diamine)_2]$ for the platinum(II) complexes and $[Pt(OH)_2(H_2P_2O_7)(diamine)_2]$ for the platinum(IV) complexes. Note that we were unable to record the limiting chemical shift values at lower pHs because of the very limited solubility of these complexes and faster acid-catalyzed hydrolysis at lower pHs. Therefore, pK_{a1} values are estimates based on the best fits of pH−δ profiles according to eq 1. The computer fits also yielded limiting chemical shifts for the completely protonated and monoprotonated species. In some case, the data were fitted to a monophasic profile according to eq 2 because of the absence of prominent biphasic features. These pK_a values and the limiting chemical shifts of the protonated forms are also listed in Table 2.

^{195}Pt NMR spectra were only recorded at neutral pH because of their increased solubility and stability. These complexes displayed shifts in the range −1503 to −1729 ppm for the platinum(II) complexes and 1582 to 1733 ppm for the platinum(IV) complexes. These chemical shifts were more downfield compared to *cis*-dichloroamineplatinum(II) compounds. No couplings between ^{195}Pt and ^{31}P NMR can be seen in these spectra because of the fact that the average line widths of these complexes far exceed the estimated coupling constants reported above.

Crystal Structure. Two platinum(IV) compounds (am-4 and en-4) and a dinuclear platinum(II) compound (dinuclear-dach-2) were characterized by X-ray crystallography. Figures 4–6 show the structures of these compounds. The unit cell information and refinement details are reported in Table 3. The atomic positions and equivalent isotropic displacement parameters and selected bond lengths are listed in Tables ST3 and ST4 in the Supporting Information. All of the Pt−O distances (1.994−2.086 Å) are within the normal single-bond range, close to the sum of the covalent radii of Pt (1.30 Å in the Pauling scale) and O (0.66 Å). In am-4 (Figure 4), there are two Na^+ ions per formula that balance the charge of the pyrophosphate group. These ions are from the starting reactant sodium pyrophosphate. In addition, there are four water molecules (OW for the water O atom in Figure 4) per formula. They have larger thermal ellipsoids because they are more labile than the atoms in the molecule. There is an extended hydrogen-bonding network propagating in the structure, connecting the ammine groups, water molecules, and the O^- group in the pyrophosphate part of the molecule. The hydroxyl groups attached to the platinum(IV) center also form multiple hydrogen bonds with ammine and O^- groups of neighboring molecules. For this reason, the positions of the H atoms on the hydroxyl groups could not be determined.

The asymmetric unit of en-4 contains two molecules (Figure 5). These two molecules have different chirality. In molecule 1, one phosphorus atom [P(11)] is above the N(11)−N(12)−O(104)−O(103) equatorial plane and the other [P(12)] is below. In molecule 2, the two P atoms have inverted geometry. The enantiomeric relationship of these two molecules is only destroyed by the different orientations of the H atoms of the hydroxyl groups attached the to the Pt atoms. However, because these H atoms are added according to the riding model of the refinement procedure, their positions cannot be used as criteria for the enantiomeric conformations of the two molecules. The heavy atoms Pt and P of these two molecules are related by a pseudosymmetry element, producing an apparent space group $Pna2_1$. Refinement in this space group would result in an unusually large thermal ellipsoid for the O atom connecting the Pt and P atoms, and the corresponding O−P distance would be close to 2 Å. Because of the packing of the molecules in the unit cell, each hydroxyl group attached to the platinum(IV) center forms one or two hydrogen bonds with adjacent molecules. To balance the charge, the pyrophosphate part has two hydroxyl groups. In en-4, one of the oxygen atoms [O(3)] of the pyrophosphate part is slightly disordered and therefore has a larger thermal ellipsoid. However, each hydroxyl group attached to the platinum(IV) center forms only one or two hydrogen bonds with adjacent molecules and could be located from the difference electron density map. The pyrophosphate part also has two hydroxyl groups to balance the charge.

The crystal structure of dinuclear dach-2 is significantly different from those of am-4 and en-4 in that it exhibits an extended network of hydrogen bonding. Figure 6a shows the dinuclear unit of the compound. For clarity, the four water molecules in the asymmetric unit are not plotted. These water molecules are important because all hydrogen bonds in the structure are via them. The two Pt atoms are connected through the pyrophosphate group. The Pt−Pt distance in the dinuclear molecule is 3.372 Å. This distance is much longer than the sum of the covalent radii of two Pt atoms (1.30 Å in the Pauling scale), yet the interaction is significant. The largest opening in the V-shaped molecule, measured as the distance between the two outmost C atoms in the two six-membered rings of the cyclohexanediamine groups, is approximately 7.630 Å. The molecules are stacked along the (−1, 1, 0) direction in a zigzag fashion, as shown in Figure 6b. The Pt−Pt distance between two adjacent dinuclear molecules is even shorter, 3.237 Å. This remarkable extended network of Pt molecules is seen only in some platinum

Table 3. Crystal Data and Structure Refinement for am-4, en-4, and Dinuclear dach-2

compound	am-4	en-4	dinuclear dach-2
empirical formula	$H_{16}N_2Na_2O_{13}P_2Pt$	$C_2H_{12}N_2O_9P_2Pt$	$C_{12}H_{25}N_4O_{11}P_2Pt_2$
fw	555.16	465.17	853.48
temperature (K)	293(2)	223(2)	203(2)
wavelength (Å)	0.71073	0.71073	0.71073
cryst syst	triclinic	monoclinic	triclinic
space group	$P\bar{1}$ (No. 2)	*Pc* (No. 7)	$P\bar{1}$ (No. 2)
unit cell dimens			
a (Å)	7.0849(6)	9.2368(9)	9.0849(7)
b (Å)	9.3445(8)	11.869(1)	10.1411(8)
c (Å)	10.5424(9)	13.335(1)	15.648(1)
α (deg)	99.611(1)	90	106.836(1)
β (deg)	91.770(1)	133.843(1)	106.251(1)
γ (deg)	103.123(1)	90	92.492(1)
volume ($Å^3$)	668.5(1)	1054.4(2)	1312.5(2)
Z	2	4	2
density(calcd) (Mg/m^3)	2.758	2.930	2.160
abs coeff (mm^{-1})	10.868	13.650	10.820
θ range for data collection (deg)	1.96−25.00	3.06−24.99	1.43−25.00
reflns collected	4991	7441	9546
indep reflns	2337 [*R*(int) = 0.0222]	3533 [*R*(int) = 0.0176]	4555 [*R*(int) = 0.0311]
completeness to *θ* = 25.00° (%)	99.3	99.3	98.8
rel max and min transmn	1.000 and 0.126 523	0.2641 and 0.1068	1.000 and 0.123 840
data/restraints/param	2337/0/188	3533/2/287	4555/0/281
GOF on F^2	1.138	1.023	1.225
final *R* indices [$I > 2\sigma(I)$]			
R1	0.0233	0.0183	0.0506
wR2	0.0633	0.0457	0.1360
R indices (all data)			
R1	0.0233	0.0200	0.0521
wR2	0.0633	0.0463	0.1367
largest diff peak and hole (e $Å^{-3}$)	1.725 and −1.794	0.637 and −0.698	2.725 and −1.372

polymeric structures such as the $Pt(CN)_4^{2-}$ chain of a number of tetracyanoplatinate compounds.[37]

The surprising observation in the crystal structure that the core Pt atoms in the dinuclear dach-2 lie only 3.24 Å apart, and thus appear to be bonded, led us to examine it computationally. Optimization (BLYP/LANL2DZ) of the model complex where 1,2-ethanediamine was substituted for cyclohexanediamine converged to a similar structure, with the core Pt atoms 3.100 Å apart. However, examination of the frontier orbitals clearly indicated that no bonding electron density lies between the two Pt atoms (Figure SF1 in the Supporting Information).

Closer inspection of the optimized structure suggested that the monomers were linked by strong hydrogen bonds between the amine H atoms and the Pt-bound pyrophosphate O atoms, with O−H distances of 1.831 and 1.929 Å and N−O distances of 2.848 and 2.888 Å. The unusual collection of four hydrogen bonds at the core of the dinuclear unit provided a means to assess their strength. The difference in energy between the dimer and two separately optimized monomer units proved to be 235 kJ mol^{-1}, suggesting an average hydrogen-bonding energy of ca. 58 kJ mol^{-1}. Obviously, this average does not reflect the molecular geometry in detail because the hydrogen-bonding distances differ by nearly 0.1 Å.

Because hydrogen bonds typically afford ca. 20−40 kJ mol^{-1} of stabilization, the value above appears anomalously large. Moreover, the presence of short O−H distances does not prove the presence of hydrogen bonds. We probed these issues computationally in three ways. First, we reoptimized the structures using the MPW1K and MP2 models, both of which have been shown to describe dispersion effects and hydrogen bonding more accurately than the pure DFT BLYP model. We also calculated the MP2 energy using the optimized BLYP structure, to examine optimization/energy effects. In each case, the dimer/two monomer energy difference was larger than that for BLYP, ranging from 288 kJ mol^{-1} (MPW1K) to 359 kJ mol^{-1} (MP2//BLYP) to 369 kJ mol^{-1} (MP2). If these values reflect the experimental value accurately, they attest to a remarkable degree of stabilization due to hydrogen bonding. However, it is possible that *all* of these methods overestimate the hydrogen-bonding energy for this complex.

We have also examined the effect of removing the hydrogen bonds through several approaches. First, the hydrogen-bonding H atoms were replaced by methyl groups, and the dimer was optimized. In a separate optimization, the H atoms were replaced by F atoms. In both cases, the monomer moieties rapidly separated, with the Pt−Pt distance growing to >4 Å within a few optimization steps. This supports the view that hydrogen bonding holds the monomers together. However, one could argue that the methyl groups/fluoride ligands push the monomers apart because they are sterically more demanding than the H atoms. This, in turn, implies that the Pt−Pt bond energy, if extant, is approximately the same as the steric repulsion energy. Thus, in a third optimization, the geometry of the hydrogen-bonding

(37) (a) Krogmann, K.; Hausen, H. D. *Z. Anorg. Allg. Chem.* **1968**, *358* (1−2), 67–81. (b) Krogmann, K.; Hausen, H. D. *Z. Naturforsch., Teil B: Anorg. Chem., Org. Chem., Biochem., Biophys., Biol.* **1968**, *23* (8), 1111. (c) Krogmann, K.; Ringwald, G. *Z. Naturforsch., Teil B: Anorg. Chem., Org. Chem., Biochem., Biophys., Biol.* **1968**, *23* (8), 1112.

H atoms was fixed such that the O−N−H angle was ca. 90°, thus making "face-to-face" hydrogen bonding of the type seen in **5** impossible. In this case, separation of the monomers to a Pt−Pt distance > 4 Å required over 20 steps but was achieved. Interestingly, in this optimization, it became clear that the monomers were shifting vertically with respect to each other so that the "fixed" H atoms could form hydrogen bonds with the uncoordinated pyrophosphate O atoms. This indicates strongly that hydrogen bonding is the main force holding the monomers together in dinuclear dach-2.

Finally, the core Pt atoms were replaced by Hg atoms, on the theory that no $d^{10}-d^{10}$ Hg → Hg bond could possibly form. Thus, if the monomers remained in proximity, the interaction holding them in place must come from another source, e.g., hydrogen bonding. In the event, the model optimized toward a system with pyrophosphate O atoms bridging the Hg atoms. However, the Hg atoms remained within 3.65 Å of each other, and the orientation of the hydrogen-bonding H atoms toward the O atoms remained as well. Thus, the computational data clearly support that dinuclear dach-2 contains no Pt−Pt interaction of any consequence and is held together by four hydrogen bonds emanating from the amine H atoms to the Pt-bound pyrophosphate O atoms.

Discussion

Mononuclear Platinum(II) and Platinum(IV) Pyrophosphato Complexes and Their NMR and X-ray Structural Characterization. Although mononuclear platinum(II) pyrophosphate complexes were readily formed and were stable for many days at neutral pH, isolation of these complexes as pure solid was proven to be extremely difficult. For example, the original method[13] of isolation for the compound by absorbing the anionic pyrophosphato compounds on an anion-exchange resin at neutral pH and eluting them with a lower pH eluant was proven to be unsuccessful for the other amine ligands. In all cases, these compounds decomposed on the ion-exchange beds when separation was attempted by elution with a lower pH electrolyte. Initially, these compounds turned brownish black, followed by the formation of an insoluble black precipitate inside the ion-exchange resins. Successful separation was only possible when the reaction mixture was concentrated by vacuum evaporation and then by a sudden change of the pH to 1.0 with nitric acid by taking advantage of the difference in solubility between the protonated and deprotonated forms of the complexes. In addition, care must be taken to reduce the volume to the extent that unreacted pyrophosphoric acid must not precipitate out when the pH is lowered because the solubility of the pyrophosphate ligand also varies greatly with the pH. On the other hand, prolonged exposure of the pyrophophato complexes to low pH solutions afforded deligation by the acid-catalyzed hydrolysis of the platinum complex as detailed below. In fact, we were unable to isolate the 1,2-ethanediamine complex perhaps because of rapid hydrolysis at low pH. Therefore, the reaction mixture must be concentrated to a critical volume to avoid either coprecipitation of pyrophosphoric acid or deligation to yield undesired platinum products.

The Pt−O and Pt−N bond distances for the two platinum(IV) complexes appear to be within the expected range of values based on the covalent radii argument of the participating atoms. However, there is a slight departure from linearity in the ∠O−Pt−O bonds for the coordinated OH^- group. The ammine compound showed an angle of 177°, while the en compound exhibited 175°. Furthermore, cis angles for the am compound, ∠O−Pt−O, ∠O−Pt−N, and ∠N−Pt−N, vary between 85° and 98°; the most severe departures were observed for the two O atoms of the pyrophosphato ligand. This deviation is 5° larger than those observed for the cobalt(III) β,γ-triphosphato six-membered chelate ring.[38] In fact, this deviation is about 3° larger than an eight-membered cobalt(III) α,γ-triphosphato complex.[39] Naturally, this expansion in the bite angle resulted in a negative deviation in the N−Pt−N angle. For the en complex, these departures were even more pronounced. The phosphate groups are arranged in a staggered configuration in the 1,2-ethanediamine complex, while an eclipsed conformation was observed for the ammine compound.

Mechanism of Formation, Structures of Pyrophosphate-Bridged Dimer and the Nature of the Extended Structure. Our NMR data can be used to address the mechanism of formation of the dinuclear complexes in an acidic solution. Because the deligation process of the pyrophosphate ligand was not accompanied by the formation of a monodentate pyrophosphato complex as evidenced by the absence of doublets in the ^{31}P NMR spectra, it is reasonable to conclude that monodentate complex formation is the rate-limiting process, followed by complete deligation. Such a deligation process would be expected to afford a diaminediaquaplatinum(II) species. A rapid reaction between the diaqua species and the starting mononuclear complex would yield the insoluble dimer. Scheme 1 shows the formation of the dimer by an acid-catalyzed hydrolysis reaction.

A number of interesting features of the bridged dinuclear complex deserve elaboration. First, the pyrophosphate anion serves as the tetradentate bridging ligand between the two Pt atoms. Second, two dinuclear units are stacked on each other in a head-to-tail fashion; i.e., pyrophosphates of the two adjacent dinuclear units are located on the opposite sides of the plane. This head-to-tail configuration repeated throughout the stack, yielding a quasi-one-dimensional planar zigzag structure. It appears that this extended structure is supported by hydrogen bonds. The head-to-tail configuration must not be confused with that described for a number of tetrameric platinum blues, including pyridone and pyrrolidone ligands, where such a configuration exists within each dinuclear

(38) Merritt, E. A.; Sundaralingam, M.; Cornelius, R. D.; Cleland, W. W. *Biochemistry* **1978**, *17*, 3274–3278.
(39) (a) Merritt, E. A.; Sundaralingam, M.; Cornelius, R. D. *J. Am. Chem. Soc.* **1980**, *102*, 6153–6154. (b) Merritt, E. A.; Sundaralingam, M.; Cornelius, R. D. *Acta. Cryst., Sect. B: Struct. Cryst. Cryst. Chem.* **1981**, *B37* (3), 657–659.

Scheme 1. Proposed Mechanism of Formation of a Pyrophosphate-Bridged Dinuclear Platinum Complex

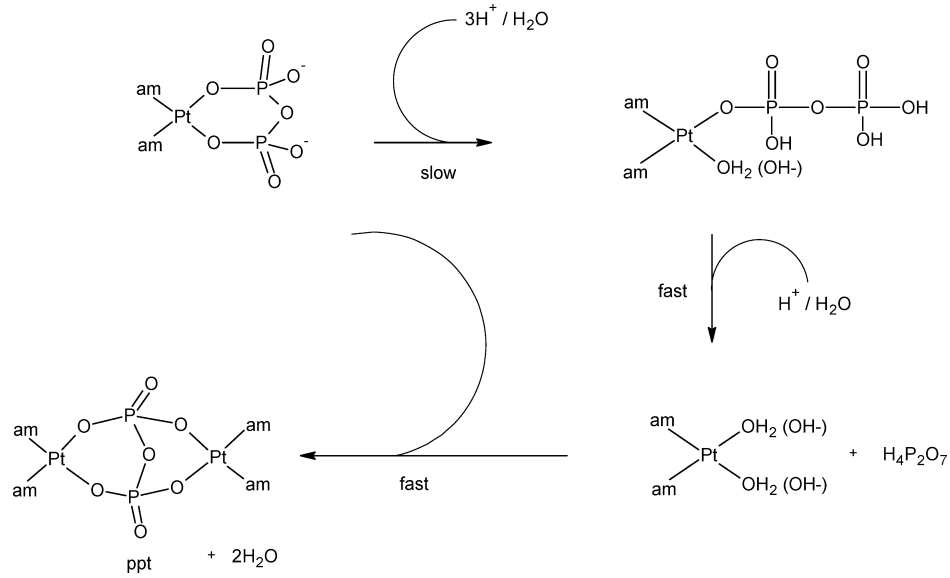

unit.[40] In fact, four hydrogen bonds between the two adjacent dinuclear units can easily be justified from the structural parameters and theoretical calculations. Third, two zigzag chains are juxtaposed in a fashion supported by additional hydrogen bonds reminiscent of DNA structures where two strands of DNA bases are held by hydrogen bonds.

Pt−Pt bond formation within a dinuclear pyrophosphate-bridged complex containing the diammine moiety was described by Stanko[12] in which a Pt−Pt bond distance of 3.22 Å was noted. The Pt−Pt bond distance for our compound, 3.37 Å, is significantly higher than that observed by Stanko. This interatomic distance, however, is substantially longer than those usually documented for Pt−Pt single and multiple bonds[41,42] and the sum of the van der Waals radii of the Pt^{2+} cation. This larger intraplatinum distance within a dimer is much larger than those of other dimers bridged by a variety of bridging ligands including α-pyridone,[41,43] pyrrolidone[44] amide,[45] thymine,[46] and uracil,[47,48] where Pt−Pt distances lie in the range 2.82−2.98 Å. In the present case, the larger Pt−Pt distance may be due to the restrictions imposed by the bridging pyrophosphate ligand. Furthermore, the dihedral angle between the adjacent planes within each dimer (44.4°) is larger than those observed for platinum complexes containing N−O bidentate chelating ligands.

The interplatinum distance between the two adjacent dinuclear units in our compound is 3.237 Å. Also, this distance is shorter than the intraplatinum distances within a dinuclear unit discussed above. Furthermore, this interplatinum distance is significantly shorter than the self-stacking of square-planar infinite chains such as Magnus green salt[49] and *cis*-$PtCl_2(NH_3)_2$.[50] Crystal structures of a number of platinum dimers with N−O donors reveal interatomic platinum distances between 3.1 and 5.6 Å.[51] The shorter interatomic distance is usually observed where the presence of significant hydrogen bonding has been demonstrated. Gray and co-workers[52] have analyzed the Pt−Pt distance in linear-chain platinum(II) diimine complexes by considering three factors: interligand steric repulsions, interligand charge-transfer bonding, and Pt−Pt bonding. The shorter Pt−Pt distances were attributed to a strong-field ligand and π-donor−acceptor characteristics of the ligand. Because pyrophosphate is not known to have π-bonding characteristics and that the dach ligand is significantly bulkier than ammine, in the present case, this shorter distance may not be due to a weak Pt−Pt bond. On the basis of molecular mechanics modeling of nonbonded interactions, Hambley[53] has estimated a van der Waals radius of Pt of about 1.7 Å. Although exact van der Waals contact for the dinuclear compound on hand would require reliable force-field parameters for pertinent bond angles, it suffices to say that the dinuclear-dach-2 compound is primarily due to the formation of hydrogen bonds between the adjacent dimers, which is supported by the DFT calculations.

(40) Hollis, S. H.; Lippard, S. J. *J. Am. Chem. Soc.* **1983**, *105*, 3494–3503.
(41) Barton, J. K.; Best, S. A.; Lippard, S. J.; Walton, R. A. *J. Am. Chem. Soc.* **1978**, *100*, 3785–3788.
(42) Roundhill, D. M.; Gray, H. B.; Che, C. M. *Acc. Chem. Res.* **1989**, *22*, 55–61.
(43) O'Halloran, T. V.; Roberts, M. M.; Lippard, S. J. *J. Am. Chem. Soc.* **1984**, *106*, 6427.
(44) Matsumato, K.; Miyamae, H.; Moriyama, H. *Inorg. Chem.* **1989**, *28*, 2959.
(45) Matsumoto, K.; Arai, S.; Ochaioi, M.; Chen, W.; Nakata, A.; Nakai, H.; Kinoshita, H. *Inorg. Chem.* **2005**, *44*, 8552–8560.
(46) Micklitz, W.; Renn, O.; Schoellhorn, H.; Thewalt, U.; Lippert, B. *Inorg. Chem.* **1990**, *29*, 1836–1840.
(47) Troetscher, G.; Micklitz, W.; Schoellhorn, H.; Thewalt, W.; Lippert, B. *Inorg. Chem.* **1990**, *29*, 2541–2547.
(48) Mascharak, P. K.; Williams, I. D.; Lippard, S. J. *J. Am. Chem. Soc.* **1984**, *106*, 6424.
(49) Cox, E. G.; Pinkard, F. W.; Wardlaw, W.; Preston, G. H. *J. Chem. Soc.* **1932**, 2527–2535.
(50) Milburn, M. G.; Truter, M. R. *J. Chem. Soc. A* **1966**, 1609.
(51) For example, see: Matsumoto, K.; Sakai, K. *Adv. Inorg. Chem.* **2000**, *49*, 375–427.
(52) Connick, W. B.; March, R. E.; Schaefer, W. P.; Gray, H. B. *Inorg. Chem.* **1997**, *36*, 913–922.
(53) Hambley, T. W. *Inorg. Chem.* **1998**, *37*, 3767–3774.

There has been tremendous interest in developing metal complexes of one-dimensional infinite chains for catalysis.[54,55] In fact, polynuclear platinum complexes have been utilized in olefin oxidation because of their ability to reversibly navigate between a number of oxidation states.[56] We have utilized a polymeric platinum phosphate complex for oxygen reduction for fuel cell applications by reductive electropolymerization.[57,58] The insoluble nature of this platinum(II) pyrophosphato complex can be exploited as an electrocatalyst for efficient oxygen reduction.

Supporting Information Available: Figure and four tables that describe the model compound for the dinuclear dach-2 compound, Cartesian coordinates, atomic coordinates and equivalent isotropic displacement parameters for the am-4, en-4, and dinuclear dach-2 compounds, and selected bond lengths and bond angles. This material is available free of charge via the Internet at http://pubs.acs.org.

IC800237A

(54) Saeki, N.; Nakamura, N.; Ishibashi, T.; Arime, M.; Sekiya, H.; Ishihara, K.; Matsumato, K. *J. Am. Chem. Soc.* **2003**, *125*, 3605–3616.
(55) Ochiai, M.; Lin, Y.-S.; Yamada, J.; Misawa, H.; Arai, S.; Matsumato, K. *J. Am. Chem. Soc.* **2004**, *126*, 2536–2545.
(56) Matsumato, K.; Ochiai, M. *Coord. Chem. Rev.* **2002**, *231*, 229–238.
(57) Bose, A.; Sarkar, M.; Bose, R. N. *J. Power Sources* **2006**, *157*, 188–192.
(58) Bose A.; Bose, R. N. Bifunctional Electrocatalyst for Fuel Cells. U.S. Patent and Trademark Office, 2007, Provisional Application 60/892,958,